MODELING THE BURNING OF COMPLICATED OBJECTS USING LAGRANGIAN PARTICLES

Kevin McGrattan, Randall McDermott, William Mell, Glenn Forney
National Institute of Standards and Technology, Gaithersburg, Maryland, USA

Jason Floyd
Hughes Associates, Inc., Baltimore, Maryland, USA

Simo Hostikka and Anna Matala
VTT Research Centre, Finland

ABSTRACT

A methodology is described for representing complicated objects within a computational fluid dynamics model. These objects are typically collections of similar items that are too small to define on the numerical grid that is used to solve the governing flow equations. Examples include vegetation like leaves and grasses, electrical cables, office clutter, and wooden cribs used in fire experiments. The basic idea is to use Lagrangian particles that are not tied to the numerical grid as a means of representing the small items. The particles can take on simple shapes like spheres, cylinders or plates, and detailed material properties can be assigned to them. A basic outline of the method and some examples are presented.

INTRODUCTION

Throughout the development of computational fluid dynamics (CFD) models of fire, it has typically been assumed, for the sake of simplicity, that solid fuels are relatively simple in geometry. In particular, it is assumed that the interface between the gas and the solid is either flat or of such a shape that thermal penetration in depth can be treated as one-dimensional. Detailed three-dimensional models of solid phase pyrolysis do exist, but they are too time-consuming to implement in a general-purpose, large-scale fire model. The assumed simplicity of the solid geometry is consistent with, and benefits from, standard bench-scale test methods and corresponding mathematical models. The simple geometries have allowed for the development of fairly sophisticated models that consider multiple layers of multi-component solids undergoing multiple chemical reactions.

However, many objects of interest in fire simulations are very complicated. In CFD parlance, these objects do not conform to the underlying numerical grid. Typically, they are treated as bulk objects of equivalent mass and thermal properties, but this is not a particularly satisfying approach and leads to inconsistent results modeler to modeler. A potential approach for treating complicated fuels is to model them as collections of particles that are not rigidly tied to the numerical grid. This approach is already used to treat fuel and water droplets, and it is proposed that the method be generalized to treat a wider class of objects. Three examples of current interest to the authors are electrical cables, vegetation, and wood cribs/pallets. At first glance, these objects do not seem to have any commonality, but given that all are potential fuels in a fire simulation, it is worth developing a general framework for representing them in a model. Recently, the pyrolysis model within the Fire Dynamics Simulator (FDS) has been generalized so that the detailed multi-component, multi-layered, multi-reaction algorithm can be applied to collections of Lagrangian particles with assumed shapes, such as cylinders, spheres or plates. Thus, complicated fuels can be approximated as point sources of mass, drag, heat release, and

radiative absorption and emission. Their effect on the gas-phase conservation laws comes via bulk source terms determined by summing the contributions of all the fuel elements. The key point is that the spatial distribution of the heat release rate must be captured in the model, along with the total heat release rate.

For example, a tray filled with electrical cables can be modeled as a collection of short cylinders with the same diameter as the cable and a length that is comparable to that of the underlying numerical grid. This last requirement is necessary because the convective and radiative heat flux from the gas to the solid is only as spatially resolved as the underlying grid. Similarly, trees and brush can be modeled as collections of small spheres, cylinders, or plates depending on the nature of the particular species. A wood crib is essentially a lattice of regularly spaced fuel "elements."

The development of models to treat the interaction of droplets with the gas phase flow field can be generalized to include these classes of objects. Because the complicated fuels can be modeled as particles, appropriate drag laws can be used to model the flow of gases around and through the objects, something that is currently impossible when treating these objects as completely solid. In addition, the particles representing the objects can absorb and emit thermal radiation. In particular, the exchange of radiation between the particles themselves is a critical part of modeling cables, wood cribs, etc., especially where surface temperatures due to charring are relatively high.

The methods being developed here have characteristics similar to other Lagrangian particle methods such as the material point method (MPM) for structural mechanics and probability density function (PDF) methods for turbulent reacting flows. The computational machinery required of these methods - particle tracking, for example - will ultimately make it possible to handle processes such as melting (often the precursor of pool fires) and fire-brand transport (a key mechanism in the spread of wildfires). Another issue is the visualization of the complicated fuels. It is challenging to depict these objects in a way that conveys to the viewer the actual appearance of the object but still represents it in a form that is faithful to the underlying assumptions. In other words, it would be deceiving to render on the computer screen a photo-realistic, three-dimensional representation of a tree, but it would also be confusing simply to render a cluster of dots. Research is currently underway to find an appropriate balance between the two extremes that will satisfy the needs of both the model developers and the end users.

Examples of the technique will be presented, along with comparisons to full-scale experiments involving electrical cables and fir trees. Of particular interest is the number of empirical parameters needed to model real fuels and the experimental apparatus available to obtain this information. The hope is that current developments in pyrolysis modeling can be applied equally well to relatively large, simple objects, like wall linings, as well as complicated fuels. In other words, with this approach we hope to avoid having to develop a new pyrolysis model for each class of complicated objects.

NUMERICAL APPROACH

Heat Transfer to and from Partlces

Most CFD models use Lagrangian particles to represent droplets, particulate matter, or any number of substances that are unresolvable on the grid but cannot be considered part of the gas phase. In the Fire Dynamics Simulator (FDS), Lagrangian particles have been used to represent sprinkler water droplets, liquid fuel droplets, and tracer particles. These droplets/particles were considered either thermally-thin (that is, they heat up uniformly) or massless. The handling of radiation absorption, emission, convective heat transfer, evaporation, *etc.*, was based on this assumption of that the particles and droplets are small, thermally-thin spheres. However, if the methodology is to be expanded to include items like tree leaves and electrical cables, the thermally-thin assumption may no longer hold. Given that the description of solid materials within FDS has become fairly detailed over the past decade, it made sense to apply general

surface boundary conditions to these Lagrangian elements in addition to large objects that are resolved on the numerical grid. In FDS, each particle class can be assigned a surface type in much the same way as is done for solid obstructions that conform to the numerical grid. The particle is assumed to be thermally-thick, but for simplicity the heat conduction within the particle is assumed to be one-dimensional in either a cylindrical, spherical or cartesian coordinate system.

It is assumed that the particles interact with the surrounding gas via an additional source term in the energy conservation equation. For a grid cell with indices ijk, the source term is:

$$(-\nabla \cdot \dot{\mathbf{q}}_r'')_{ijk} = \sum \left[\kappa_p \left(U_{ijk} - 4\sigma T_p^4 \right) \right] \tag{1}$$

where the summation is over all the particles within the cell. The term U_{ijk} is the integrated intensity of the grid cell, and $\dot{\mathbf{q}}_r''$ is the radiation flux vector. It is the discrete analog of the term:

$$U(\mathbf{x}) = \int_{4\pi} I(\mathbf{x}, \mathbf{s}')\, d\mathbf{s}' \tag{2}$$

and $I(\mathbf{x}, \mathbf{s})$ is the radiation intensity, a function of the spatial coordinate, $\mathbf{x}$, and solid angle, $\mathbf{s}$. The particle surface temperature, T_p, is used in the computation of the radiative emission. Equation (1) defines the role of the particles in the absorption and emission of radiant energy from a given grid cell. The effective absorption coefficient for a single particle is given by

$$\kappa_p = \frac{A}{4V_{ijk}} \tag{3}$$

where A is the surface area of the particle and V_{ijk} is the volume of the cell. The net radiative heat flux onto the surface of the particle is

$$\dot{q}_{r,p}'' = \varepsilon \left(\frac{U_{ijk}}{4} - \sigma T_p^4 \right) \tag{4}$$

and the net convective heat flux is

$$\dot{q}_{c,p}'' = h(T_{ijk} - T_p) \tag{5}$$

where h is the convective heat transfer coefficient appropriate for the particular particle shape and T_{ijk} is the local gas temperature. This approach for transferring energy between the particle and the gas phase is similar to techniques for modeling objects such as thermocouples[1].

Pyrolysis Model

The value of the Lagrangian particle approach for items that can burn is that the pyrolysis model applied to the object can be fairly detailed and involve multiple layers and multiple material components. If these objects must conform to a uniform numerical grid (as in past versions of FDS), it is rather awkward to apply detailed pyrolysis models because the error associated with the geometry makes a detailed pyrolysis model unwarranted.

This section describes a method of determining and applying the values of the kinetic parameters for the thermal decomposition of a solid, following the methodology described by Lyon[2]. Consider a solid material that undergoes multiple reactions during its thermal decomposition. Looking at the results of a thermal gravimetric analysis (TGA), for example, it is possible to identify peaks in the reaction rate curve corresponding to temperature ranges over which most of the mass loss occurs. From this measurement alone, it is not possible to determine the chemical make-up of the solid. However, if it is assumed that the number of material components making up the solid is equal to the assumed number of reactions, as determined from the TGA results, the mass fraction of any component, $Y_i(t)$, can be modeled according to the equation:

$$\frac{dY_i}{dt} = -A_i Y_i \exp\left(-\frac{E_i}{RT} \right) \quad ; \quad Y_i(0) = Y_{0,i} \tag{6}$$

In the TGA apparatus, the temperature of the sample is increased linearly in time, $dT/dt = \beta$. Because TGA results are usually expressed as a function of temperature rather than time, it is convenient to rewrite Eq. (6) as:

$$\frac{dY_i}{dT} = -\frac{A_i}{\beta} Y_i \exp\left(-\frac{E_i}{RT}\right) \quad ; \quad Y(T = T_0) = Y_{0,i} \tag{7}$$

The decomposition rate, $-dY_i/dt$, peaks at a temperature denoted by $T_{p,i}$ with a value denoted by $r_{p,i}$. At this temperature, the second derivative of Y_i is zero:

$$\frac{d^2Y_i}{dT^2} = -\frac{A_i}{\beta}\frac{dY_i}{dT}\exp\left(-\frac{E_i}{RT_{p,i}}\right) - \frac{A_i}{\beta} Y_i \exp\left(-\frac{E_i}{RT_{p,i}}\right)\frac{E_i}{RT_{p,i}^2} = -\frac{dY_i}{dT}\left[\frac{A_i}{\beta}\exp\left(-\frac{E_i}{RT_{p,i}}\right) - \frac{E_i}{RT_{p,i}^2}\right] = 0 \tag{8}$$

Next, Eq. (7) can be integrated from $Y_{0,i}$ to $Y_{p,i}$ (the value of Y_i at the peak), and T_0 to $T_{p,i}$:

$$\int_{Y_{0,i}}^{Y_{p,i}} \left(\frac{dY_i'}{Y_i'}\right) = -\frac{A_i}{\beta}\int_{T_0}^{T_{p,i}} \exp\left(-\frac{E_i}{RT'}\right) dT' \approx -\frac{A_i RT_{p,i}^2}{\beta\,(E_i + 2RT_{p,i})}\exp\left(-\frac{E_i}{RT_{p,i}}\right) \tag{9}$$

Using Eq. (8) to eliminate A_i yields:

$$\ln\left(\frac{Y_{p,i}}{Y_{0,i}}\right) = -\frac{E_i}{E_i + 2RT_{p,i}} \approx -1 \qquad (E_i \gg 2RT_{p,i}) \tag{10}$$

or more simply, $Y_{p,i} \approx Y_{0,i}/e$. Now, the activation energy can be evaluated using Eqs. (6) and (8):

$$E_i = RT_{p,i}^2 \frac{A_i}{\beta}\exp\left(-\frac{E_i}{RT_{p,i}}\right) = \frac{RT_{p,i}^2}{\beta}\frac{r_{p,i}}{Y_{p,i}} \approx \frac{RT_{p,i}^2}{\beta}\frac{er_{p,i}}{Y_{0,i}} \tag{11}$$

Then A_i can be evaluated directly from Eq. (6):

$$A_i = \frac{r_{p,i}}{Y_{p,i}}\exp\left(\frac{E_i}{RT_{p,i}}\right) \approx \frac{er_{p,i}}{Y_{0,i}}\exp\left(\frac{E_i}{RT_{p,i}}\right) \tag{12}$$

Note that the formulae for A_i and E_i are appropriate for multiple-step reactions, where the number of peaks in the reaction rate curve is assumed to equal the number of material components, and each component is assumed to undergo a single-step reaction that forms a single fuel gas and residue. No information is provided from the TGA data alone to assume otherwise. Under these assumptions, the values of $T_{p,i}$ and $r_{p,i}$ can be obtained directly from inspection of the reaction rate curve. The values of $Y_{0,i}$ can be estimated based on the relative area underneath each peak.

What follows is an example of how to use Eqs. (11) and (12) to determine the kinetic constants for materials used in the construction of electrical control cables. However, instead of TGA, micro-combustion calorimeter (MCC) measurements are used in the analysis. The pyrolysis combustion flow calorimeter (PCFC), developed by Lyon and Walters[3] at the U.S. Federal Aviation Administration (FAA), is a device used to measure the heat generated from the combustion of small (4 mg to 6 mg) material samples by oxygen depletion calorimetry. Samples are pyrolyzed at a specified heating rate in an anerobic atmosphere (typically N_2) and the resulting gases are mixed with excess oxygen and combusted in a separate chamber. The heat release rate from the specimen is obtained from measurements of the concentration of oxygen in the effluent exiting the combustor as a function of time. The methodology is the basis for the standard test ASTM D 7309[4].

The results of PCFC measurements for the jacket and insulation material of a multi-conductor control cable are shown in Fig. 1. For each cable, the insulation and jacket material were tested separately, and at least three replicates were performed for each (only one replicate is shown for each sample). The samples, weighing approximately 5 mg, were cut from the cable jackets and conductor insulation

material of each of the cables. These samples were pyrolyzed in the PCFC at a rate of 1 K/s from 100 °C to 600 °C in a nitrogen atmosphere and the effluent combusted at 900 °C in a mixture consisting of 20 % O_2 and 80 % N_2. The resulting curve shows the heat release rate of the sample as it was heated, normalized by the mass of the original sample. There are usually one, two or three noticeable peaks in the curve, corresponding to temperatures where a significant decomposition reaction occurs. Each peak can be characterized by the maximum value of the heat release rate ($\dot{q}_{p,i}$), the temperature ($T_{p,i}$), and the relative fraction of the original sample mass that undergoes this particular reaction ($Y_{0,i}$). The area under the curve

$$\int_0^\infty \dot{q}(T)\,dT = \beta \Delta H' \tag{13}$$

is the sample heating rate (β) times the energy released per unit mass of the original sample ($\Delta H'$). This latter quantity is related to the more conventional heat of combustion via the relation

$$\Delta H = \frac{\Delta H'}{1-\nu_r} \tag{14}$$

where ν_r is the fraction of the original mass that remains as residue. Sometimes this is referred to as the "char yield." Note that it is assumed to be the same for all reactions.

The MCC measurement is similar to TGA in that it is possible to derive the kinetic parameters, A_i and E_i, for the various reactions from the heat release rate curve. As an example of how to work with MCC data, consider the two plots shown in Fig. 1. The solid curves in the figures display the results of micro-calorimetry measurements for the insulation and jacket material of a multi-conductor control cable (the number 701 has no particular meaning other than to distinguish it from other cables being studied). Both materials exhibit two fairly well-defined peaks and are modeled using two solid components, each

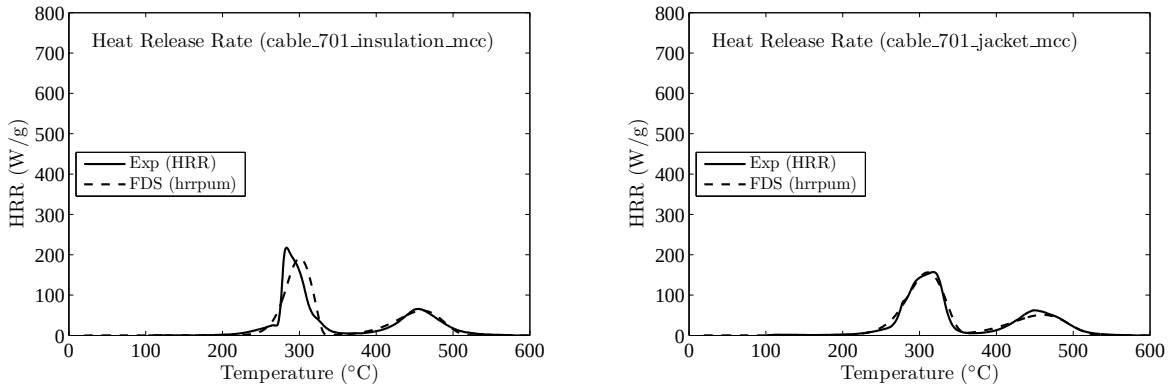

Figure 1: Results of a micro-calorimetry analysis of a sample of cable insulation (left) and jacket material (right).

undergoing a single-step reaction that produces fuel gas and a solid residue. The residue yield for the insulation material is 28 %; for the jacket 22 %, obtained simply by weighing the sample before and after the micro-calorimetry measurement. It is not known which reaction produces what fraction of the residue. Rather, it is assumed that each reaction yields the same residue in the same relative amount. The dashed curves in Fig. 1 are the results of FDS simulations of the MCC measurements. To mimic the sample heating, a very thin sheet comprised of a mixture of the solid components with an insulated backing is heated at the rate specified in the experiment (1 K/s or 60 K/min, the units needed in FDS). For each reaction, the kinetic parameters are calculated using the formulae (11) and (12). The values of $T_{p,i}$ are obtained directly from the figures. The value of $r_{p,i}$ for the ith reaction can be found from:

$$r_{p,i} = \beta \frac{\dot{q}_{p,i}}{\Delta H'} \quad ; \quad \Delta H' = \int_0^\infty \dot{q}(T)\,dT \tag{15}$$

where $\dot{q}_{p,i}$ is the value of the ith heat release rate peak. The values, $Y_{0,i}$, can be estimated from the relative area under the curve. Their sum ought to be 1.

Preliminary Results

This section describes a simulation of an experiment involving burning electrical control cables. The experiments were part of a multi-year program called CHRISTIFIRE (Cable Heat Release, Ignition, and Spread in Tray Installations during FIRE), a U.S. Nuclear Regulatory Commission Office of Nuclear Regulatory Research program to quantify the mass and energy released from burning electrical cables. One of the intermediate-scale experiments involved a single tray of cables exposed to a bank of radiant panels. The apparatus consists of a single horizontal tray with varying amounts of cable exposed to an array of quartz-faced radiant panels. The tray is 1.2 m long and 0.45 m wide. Six panels are used in two symmetric banks. The radiant panels are 25 cm by 30 cm, and produce a maximum radiant output of 4.8 kW each, or a maximum heat flux of 62 kW/m^2. See Fig. 2 for photographs of the apparatus. Preliminary measurements demonstrated that this configuration can produce approximately 30 kW/m^2 over 1 m of the cable tray. The objective of these experiments was to compile a table of heat release rates per unit area for a variety of heat flux exposures and tray loadings.

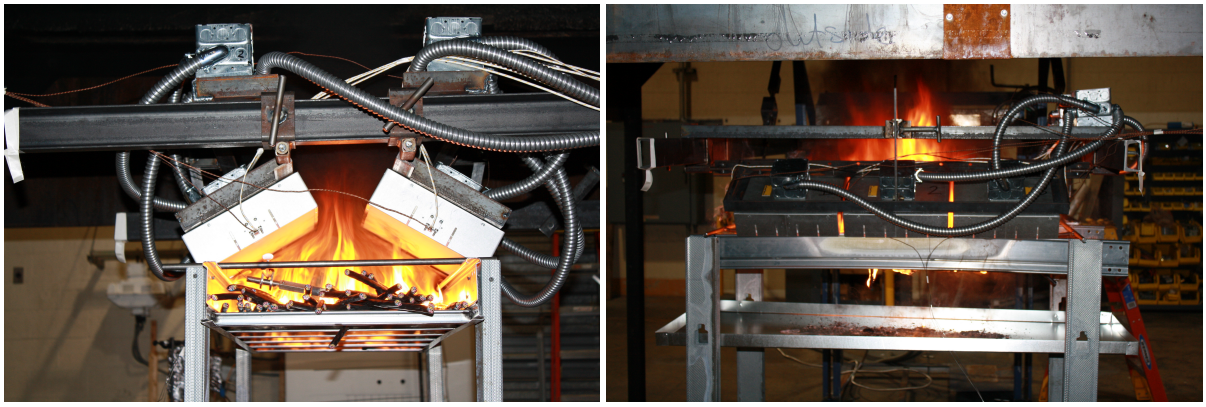

Figure 2: End and side views of the Radiant Panel Apparatus.

In order to simulate one of the cable fire experiments, a substantial amount of information is needed. First, the cables were modeled as 10 cm discrete cylindrical segments randomly arranged to partially fill the same volume as the actual cables. The cables were arranged in no particular order in the tray to mimic standard installation practice. Each segment was assumed to consist of a 1.5 mm thick jacket surrounding a mixture of copper and insulation material. Because the heat conduction calculation is only one dimensional, there is no point in trying to model individual copper conductors surrounded by insulation material, filler, and air gaps. What is most important is that the proper mass fractions are retained. In this case, the cable is 0.366 kg/m, 14 mm in diameter, and the mass fractions of copper, jacket, and insulation material are 0.58, 0.24, and 0.18, respectively. There are seven conductors in all, but this information is not of value here. The kinetic constants for the jacket and insulation material are derived from Eqs. (11) and (12). The heats of combustion for both materials is taken as 16.4 MJ/kg and the heats of reactions are all taken as 2.0 MJ/kg. These values are all taken from Tewarson's chapter of the SFPE Handbook[5]. The base materials are polyvinyl chloride (PVC), but there are plasticizers and other additives mixed in. Values for thermal conductivity, k, density, ρ and specific heat, c, were estimated from the cable literature. The project to study these cables is on-going, and more precise information on these properties is not yet available. What is more important here is not the specifics of this particular cable, but rather the fact that the particle-based approach to modeling cables allows for a fairly detailed description of it.

In addition to the cables, the gaseous fuel is assumed to be a combination of polyethylene and PVC, $C_2H_{3.5}Cl_{0.5}$. The soot yield is assumed to be 0.1, based only on the fact that the fire produced a significant amount of soot. The radiant panels were modeled as solid blocks with a surface temperature of 750 °C. Snapshots from the simulation are shown in Fig. 3. Note that the visualization program that accompanies FDS, Smokeview, has been modified to draw the cable segments, in this case colored by their surface temperature.

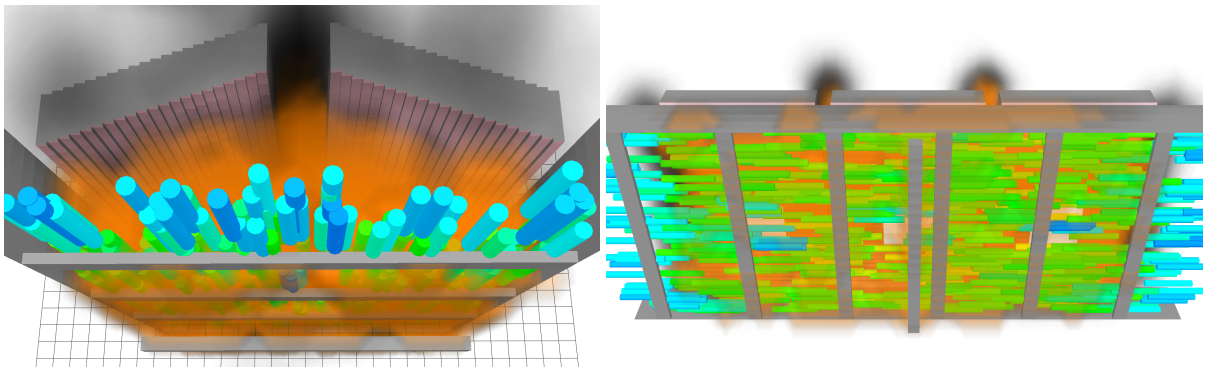

Figure 3: Visualization of the cable segments.

A comparison of the predicted and measured heat release rate is shown in Fig. 4. The results are far from perfect, and the two most obvious problems are as follows. First, the modeled cables take longer to heat up then the real cables because the heat flux to the cable is averaged over the entire circumference. This is the consequence of using the integrated intensity to calculate the flux. To improve this situation, it might be necessary to "break up" the cable into quarters so that the high heat flux from the radiant panels and low heat flux from below can be better treated. Second, this particular model of a cable does not include a comprehensive set of material properties. Even though the particle-based method of treating fuels in an improvement over the "solid slab" approach, there still remains the issue of how to obtain material properties for complex items.

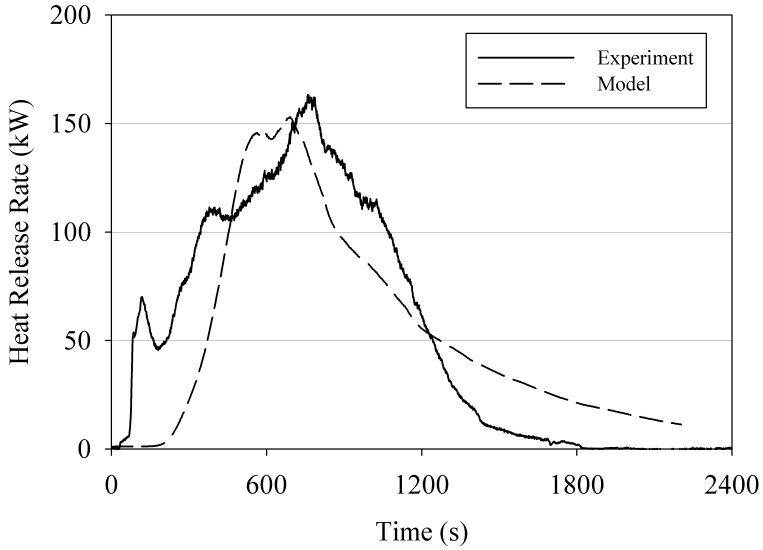

Figure 4: Comparison of predicted and measured heat release rate of burning cables in the Radiant Panel Apparatus.

BURNING TREES

This section describes an experimental and modeling study of burning trees using the basic methodology outlined above. Further details on this study can be found in Mell *et al.*[6].

Experimental Description

Tree burning experiments were conducted in the Large Fire Laboratory at NIST to use as validation data for numerical simulations. Douglas fir was selected as the tree species for these experiments because it is abundant in the western United States of America where wildland fires are most prevalent. A schematic showing the different measures used to describe a tree is shown in Fig. 5. Trees of two different

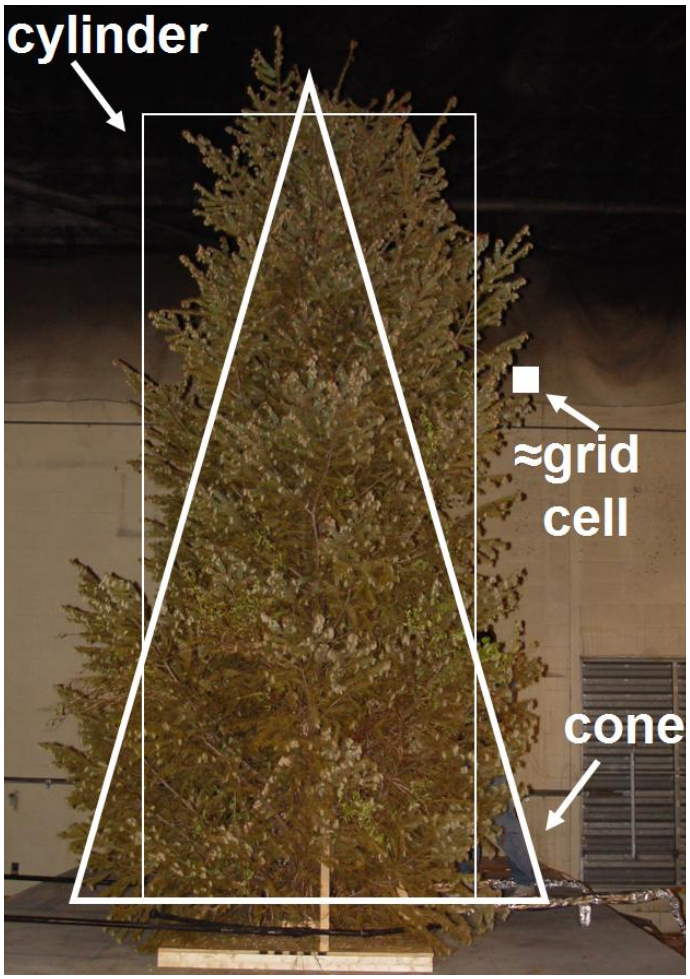

Figure 5: Photograph of 5 m tall Douglas fir with the outlines of the cross sections of both a conical and a cylindrical volume approximation to the tree crown. For simplicity the model approximates the tree as a cone or a cylinder. The approximate size of a grid cell (10 cm) is also shown.

heights were burned: approximately 2 m and 5 m. Needle samples, as well as small branch samples (three heights, four radial locations at each height), were collected for the moisture measurements. The moisture content, M, determined on a dry basis, is given as a percentage:

$$M = \frac{m_{e,\mathrm{wet}} - m_{e,\mathrm{v}}}{m_{e,\mathrm{v}}} \times 100\ \%, \tag{16}$$

where $m_{e,\mathrm{wet}}$ is the measured mass of the virgin vegetation and $m_{e,\mathrm{v}}$ is the mass of the dried virgin

vegetation; the subscript e denotes a vegetative fuel element of a given type.

Experimental measurements from nine 2 m tall Douglas fir and three 5 m tall Douglas fir were collected. By design the average moisture levels for the 2 m trees fell into three ranges: $M < 30\%$, $30\% < M < 70\%$, and $70\% < M$. Babrauskas reported that burning characteristics of Douglas fir differed according to these three levels of moisture content [7]. For $M < 30\%$ a tree ignites easily and the fire spreads relatively quickly through the crown, which is often fully consumed. Trees with $30\% < M < 70\%$ are in a transition region, successful ignition results in only partial consumption of the crown. In trees with $70\% < M$ little burning occurs beyond what is supported by the ignitor used in the experiments. The observed fire behavior in the current experiments is consistent with Babrauskas's observations. At least three replicate burns were conducted for each tree height and moisture content regime.

Model Inputs

Computer simulations of the three cases of Douglas fir burn-experiments were conducted. Details can be found in Mell *et al.* [6]. Figure 6 shows a snapshot from an experiment and characteristic simulation of a 2 m tall tree burn. The numerical model requires a number of thermo-physical properties for the gas

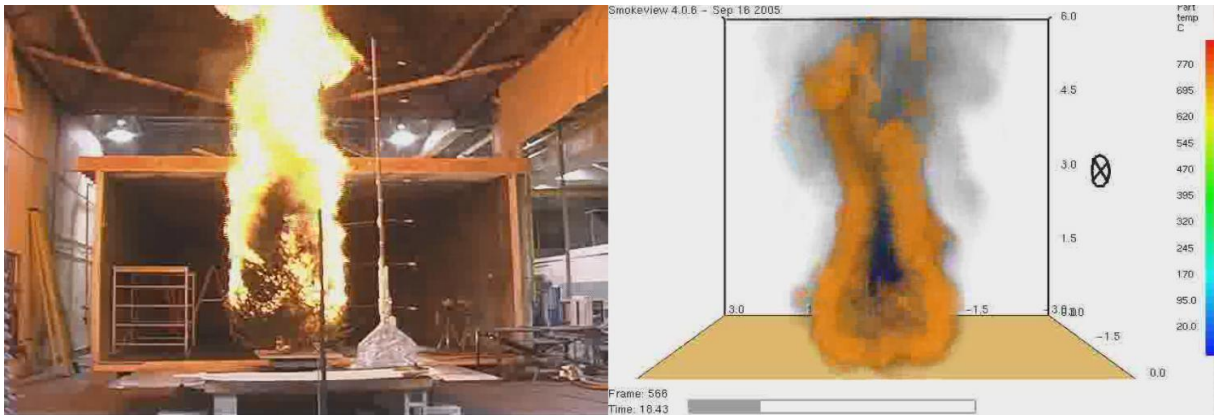

Figure 6: Experiment and simulation of a burning fir tree.

phase and the vegetative fuel. Required properties of the vegetative fuel can be categorized as follows:

Geometry: A typical CFD fire calculation can resolve something like a tree to, at best, about 10 cm. However, measuring the mass and size distribution of vegetation at this resolution would take significant effort. For simplicity, the small particles that represent the tree crown are distributed within a well-defined shape such as a cone or cylinder. This requires measured or estimated values of the width and height of the crown base, the width of the crown top, and the total height of the tree. For example, in the 2 m tall tree case the average crown base width and height are 1.7 m and 0.15 m, respectively; and the average tree height is 2.1 m. These dimensions are sufficient to represent the tree as a cone.

Bulk density The model equations require the bulk density of the dry (zero moisture) thermally thin vegetation. It was observed that, for the 5 m trees and the drier 2 m trees all foliage and roundwood up to approximately 10 mm in diameter was consumed by the fire. It was assumed that the consumption of thermally-thin vegetation (i.e., foliage and roundwood $\leq$ 6 mm in diameter) dominated this mass loss. In other words, for these relatively dry $M < 30\%$ trees, the fire pruned out the thermally thin vegetation allowing an estimation of the thermally thin mass in the crown.

Packing ratio The packing ratio, ρ_{bv}/ρ_e, is an important parameter in the drag and radiation heat trans-

fer. Its value depends on the bulk density, ρ_{bv}, and the fuel element (particle) density, ρ_e, (discussed below).

The numerical model requires the following properties of the particles that represent the needles of the tree. These are assumed to be thermally-thin.

Density: A value of $\rho_e = 514$ kg/m^3 was used for the fuel particle density[8].

Moisture: The fuel element moisture was defined to be the average of moisture (see Eq. (16)) measured from the trees for a given case. These measurements were made at a number of locations in the thermally thin fuels within the tree crowns.

Char fraction: Susott measured the char fraction for Douglas fir foliage, stems, and wood[9]. The average of these measurements, 0.26, was used here.

Specific heat: The relation for the specific heat of dry virgin Douglas fir reported by Parker[10] was used.

Surface-to-volume ratio: The surface to volume ratio (3940 m^{-1}with standard deviation of 366 m^{-1}) of the needles was obtained by averaging measured dimensions (length, width, and thickness) of 30 needles with calipers. The needle shapes were closer to flat strips than cylinders.

For the gas phase, the heat of combustion is assumed to be $\Delta H = 17.7$ MJ/kg. This is the heat released per kg of gaseous fuel, not per kg of solid fuel. It is derived from the char fraction and the average heat of combustion of volatiles measured from Douglas fir wood and foliage[9]. Note that the heat of combustion is reported in terms of energy released per unit mass of the *virgin fuel*, not the gaseous fuel. A few typical results are shown in Fig. 7

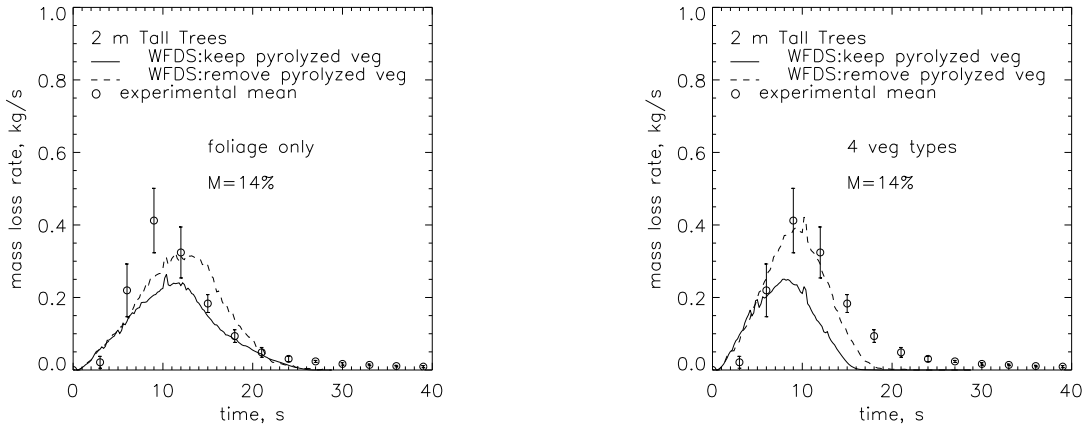

Figure 7: Figures showing the mass loss rate versus time for the 2 m tall, M = 14%, trees from the experiments and the simulations. The average mass loss rate from the six experimental burns are circles with vertical lines showing one standard deviation above and below the average. Solid and dashed lines are FDS results and distinguish between two methods of handling a fuel element after the virgin fuel has burned off leaving only char. For the solid line case the fuel element is kept as a source of drag, thermal mass, and radiative absorption/emission. For the dashed line case the fuel element is removed from the simulation. Char oxidation is not modeled in either case. In the figure on the left, the tree crown is assumed to consist solely of foliage. On the right, the tree crown consists of vegetation (fuel elements) of four different sizes, as determined from bioassay measurements.

CONCLUSION

A method of representing complicated fuels in a computational fluid dynamics model has been presented. The benefit of the approach is that it allows for a fairly detailed description of the items, and it exploits existing pyrolysis models. This is not a new pyrolysis model, but rather a better geometric description of the solids that allows for a more realistic interaction between the solid and gas phase.

The examples presented include burning cables and burning trees; two types of fuels that are very difficult to model as solid objects. As discrete particles, these items are more naturally defined by input parameters that describe the basic geometry of the objects. For example, the diameter and layer thicknesses of a cable are input directly instead of having to estimate equivalent thicknesses for a solid slab. It is hoped that eventually this approach will lead to a wider use of more detailed pyrolysis models because of the reduced need for *ad hoc* approximations related to the basic geometry.

ACKNOWLEDGMENTS

The work described in this paper was partially funded by the U.S. Nuclear Regulatory Commission and the U.S. Forest Service.

REFERENCES

1. S. Welsh and P. Rubini. Three-dimensional Simulation of a Fire-Resistance Furnace. In *Fire Safety Science – Proceedings of the Fifth International Symposium*. International Association for Fire Safety Science, 1997.

2. R.E. Lyon. Heat Release Kinetics. *Fire and Materials*, 24:179–186, 2000.

3. R.E. Lyon and R.N. Walters. Pyrolysis Combustion Flow Calorimetry. *Journal of Analytical and Applied Pyrolysis*, 71(1):27–46, March 2004.

4. American Society for Testing and Materials, West Conshohocken, Pennsylvania. *ASTM D 7309-07, Standard Test Method for Determining the Flammability Characteristics of Plastics and Other Solid Materials Using Microscale Combustion Calorimetery*, 2007.

5. A. Tewarson. *SFPE Handbook of Fire Protection Engineering*, chapter Generation of Heat and Gaseous, Liquid, and Solid Products in Fires. National Fire Protection Association, Quincy, Massachusetts, fourth edition, 2008.

6. W. Mell, A. Maranghides, R. McDermott, and S. Manzello. Numerical simulation and experiments of burning Douglas fir trees. *Combustion and Flame*, 156:2023–2041, 2009.

7. V. Babrauskas. *The SFPE Handbook of Fire Protection Engineering*. National Fire Protection Assoc., Quincy, MA, fourth edition, 2008.

8. S.J. Ritchie, K.D. Steckler, A. Hamins, T.G. Cleary, J.C. Yang, and T. Kashiwagi. The effect of sample size on the heat release rate of charring materials. pages 177–188. International Association for Fire Safety Science, March 3–7 1997.

9. R.A. Susott. Characterization of the thermal properties of forest fuels by combustible gas analysis. *Forest Sci.*, 2:404–420, 1982.

10. W.J. Parker. Prediction of the heat release rate of Douglas fir. pages 337–346. International Association for Fire Safety Science, June 13-17 1988. Hemisphere Publishing, New York.